Journal of Alloys and Compounds 498 (2010) 121–129

Contents lists available at ScienceDirect

Journal of Alloys and Compounds

journal homepage: www.elsevier.com/locate/jallcom

The structure and energetic of $AlAs_n$ (n = 1–15) clusters: A first-principles study

Ling Guo*

School of Chemistry and Material Science, Shanxi Normal University, Linfen 041004, China

ARTICLE INFO

Article history:
Received 25 November 2009
Received in revised form 20 February 2010
Accepted 28 February 2010
Available online 23 March 2010

Keywords:
$AlAs_n$ cluster
Density-functional theory
Stability

ABSTRACT

Geometric structures of $AlAs_n$ (n = 1–15) clusters are reported. The binding energy, dissociation energy, stability of these clusters are studied with the three-parameter hybrid generalized gradient approximation (GGA) due to Becke–Lee–Yang–Parr (B3LYP). Ionization potentials, electron affinities, hardness, and static polarizabilities are calculated for the ground-state structures within the same method. The growth pattern for $AlAs_n$ (n = 6–15) clusters is Al-substituted pure As_{n+1} clusters and it keeps the similar frameworks of the most stable As_{n+1} clusters (for example $AlAs_6$, $AlAs_7$, $AlAs_9$, $AlAs_{14}$ and $AlAs_{15}$ clusters) or capping the different sides of the low-lying geometry of As_n clusters (for example $AlAs_8$, $AlAs_{10}$, $AlAs_{11}$, and $AlAs_{12}$ clusters). The Al atom prefer to occupy a peripheral position for n < 12, and starting from n = 12 clusters, the Al atom completely falls into the center of the As frame. The above growth pattern is not suitable for $AlAs_n$ (n = 1–5, 13) clusters. The odd–even oscillations from $AlAs_n$ (n = 5–15) in the dissociation energy, the second-order energy differences, the HOMO–LUMO gaps, the electron affinity, and the hardness are more pronounced. The stability analysis based on the energies clearly shows the $AlAs_n$ clusters from n = 5 with an even number of valence electrons are more stable than clusters with odd number of valence electrons.

1. Introduction

Small clusters composed of arsenic atom have been the subjects of intensive studies for the last two decades. A large number of studies of arsenic clusters, both theoretical as well as experimental have been reported. (See, for example, the reviews in Refs. [1–5].) One of the main motivations behind these studies is to understand the evolution of physical properties with the size of the cluster. The question I address here is the effect of doping by a single impurity on the electronic structure and geometry of arsenic clusters. In bulk materials, a small percentage of impurity is known to affect the properties significantly. In clusters, the impurity effect should be even more pronounced and influenced by the finite size of the system. Liu et al. [6] performed some experiments in Al_nAs_m cluster. This experimental work triggered an interest in simulations of AlAs clusters. *Ab initio* calculations on properties of Al_xAs_y clusters have been carried out by several groups [7–13]. Andreoni [7] calculated the structures, stability, and melting of $(AlAs)_n$ (n = 2–5) using the Car-parrinello method. Quek et al. [8] reported tight binding molecular dynamics studies of the structures of Al_mAs_n ($m + n \leq 13$). Tozzini et al. [9] presented extensive theoretical calculations of the geometric and electronic properties of neutral and ionized AlAs fullerene-like clusters of the type Al_xAs_{x+4} with a number of atoms up to 52, on the basis of density-functional theory. Costales et al. [10] used density-functional theory (DFT) to explore structural and vibrational properties for $(AlAs)_n$ clusters up to 6 atoms, finding the same behavior as in the aluminum nitride clusters. Archibong and St-Amant [11] calculated the low-lying electronic states of Al_3As, $AlAs_3$, and the corresponding anions at the B3LYP and CCSD(T) levels of theory using the 6-311+G(2df) one-particle basis set. The adiabatic electron affinities, electron detachment energies and harmonic vibrational frequencies of both the anions and the neutral molecules are presented and discussed. Feng et al. [12] reported a MRSDCI study of the ground and several low-lying excited states of Al_2As_3, Al_3As_2, and their ions. Recently, Zhu [13] studied the spectroscopic properties for Al_2As, $AlAs_2$, and their ions using density-functional theory (DFT:B3LYP) and complete active space multiconfiguration self-consistent field (CASSCF) calculations.

To provide further insight on $AlAs_n$ clusters, I have carried out a detailed systematic study of the equilibrium structure and various electronic-structure related properties of these clusters, employing both Becke's three-parameter hybrid functional with perdew/wang 91 and Becke's three-parameter hybrid functional using the LYP correlation functional. I investigate the relative ordering of these structures with the Al impurity occupying the peripheral and other different position, and show that the ground-state structures of $AlAs_n$ (n = 1–15) have Al taking a peripheral position. The calculations are explicitly carried out, to my knowledge for the first time, by considering all electrons in the calculations with

* Tel.: +86 3572990082; fax: +86 3572990082.
E-mail address: gl-guoling@163.com.

0925-8388/$ – see front matter © 2010 Elsevier B.V. All rights reserved.
doi:10.1016/j.jallcom.2010.02.202

Table 1
Calculated bond length (Å), vibrational frequencies w (cm^{-1}), adiabatic electronic affinity AEA (eV), and adiabatic ionization potential AIP (eV), previous theoretical study and experimental results.

	As_2			Al_2	
	Our work	Theoretical	Experimental	Our work	Experimental[a]
Bond length (Å)	2.192	2.124[b]	2.103[c]	2.596	2.560
w (cm^{-1})	400.4	412[b] 394[d]	429.55[c]	289.2	350.01
AEA (eV)	0.792		0.739 ± 0.008[e]	1.39	1.55
AIP (eV)	9.712		9.69 ± 0.02[f]		

[a] Ref. [19].
[b] Ref. [2].
[c] Ref. [20].
[d] Ref. [21].
[e] Ref. [4].
[f] Ref. [3].

no pseudopotentials (with nonlocal gradient corrections). Furthermore, the all-electron treatment eliminates issues like core-valence exchange-correlation, which occurs in the pseudopotential treatment when there is no marked distinction between the core and valence regions. Here, I study the evolution of the ionization potential, electron affinity, HOMO–LUMO gap, hardness, polarizability, dissociation energy, and binding energy for $AlAs_n$ clusters up to $n = 15$. These physical quantities are compared with their counterparts calculated at the same level (all-electron B3LYP/lanl2dz) for pure arsenic clusters, which to my knowledge also represent the first all-electron with gradient corrections calculations in these systems.

In the following section, I briefly outline the computational methodology. In Section 3 the results are presented and discussed, and I conclude in Section 4.

2. Methodology and computational details

The selection of distinct initial geometries is important to the reliability of the ground-state structures obtained. As the cluster size increases, the number of the possible geometries increases dramatically. In this paper, the conformations of the pure As_n clusters are obtained by reference to the configurations in Refs. [1–5]. The geometries with different symmetries are also optimized for each size. During the course of choosing initial structures of the $AlAs_n$ clusters, I have considered possible isomeric structures by placing the Al atom on each possible site of the As_n cluster as well as by substituting one As atom by the Al atom from the As_{n+1} cluster. The Ti_nAl [14], $AlPb_n$ [15], and Sc_nAl [16] stable isomers are also considered as candidates. For all isomers of each cluster, the local minima of the potential energy surface are guaranteed by the harmonic vibrational frequencies without imaginary mode. Further, different spin multiplicities of the low-lying energy isomers are considered. In case the total energy decreases with increasing spin multiplicity, I consider an increasingly higher spin state until the energy minimum with respect to spin multiplicity is reached.

All calculations were performed using the density-functional theory (DFT) provided by the Gaussian 03 suite of programs [17]. The density functional is treated with the generalized gradient approximation (GGA) corrected-exchange potential of the B3LYP. The double-ξ basis set lanl2dz is employed [18].

The accuracy of the current computational scheme has been tested by the calculation on the As_2 and Al_2 dimer. The results are summarized in Table 1. For As_2, I obtain a bond length (2.192 Å) that fits well with the theoretical values of 2.124 Å by the MP2 [2] and 2.103 Å of experimental bond length [20]. The vibrational frequency (400.4 cm^{-1}), the adiabatic electron affinity (0.792 eV) and the adiabatic ionization potential (9.712 eV) of As_2 are also obtained, which are in good agreement with the previous theoretical and experimental values of 412 cm^{-1} [2], 394 cm^{-1} [21], 0.739 ± 0.008 eV [4], and 9.69 ± 0.02 eV [3], respectively. Additionally, the bond length (2.596 Å), vibrational frequency (289.2 cm^{-1}), and the vertical electron detachment energy (1.39 eV) of Al_2 are obtained, which are in good agreement with the experimental values of 2.56 Å, 350.01 cm^{-1}, and 1.55 eV, respectively. This indicates that our approach provides an efficient way to study small $AlAs_n$ clusters.

3. Results and discussion

3.1. Atomic structures

The ground-state geometries of $AlAs_n$ ($n = 1$–15) clusters, and some low-lying metastable isomers are shown in Fig. 1. For proper comparison I have also shown the ground-state geometries of pure As_n ($n = 2$–16) clusters, which was reported in our recent work [5]. The symmetries, the spin multiplicities, and the electronic states of the most stable $AlAs_n$ ($n = 1$–15) clusters are summarized in Table 2.

For the AlAs dimer with $C_{\infty v}$ symmetry, the optimized results indicate that the triplet spin state is lower in total energy than the singlet and quintet isomers by 0.93 and 1.47 eV, respectively. Therefore, the triplet AlAs dimer with a bond length of 2.420 Å is the most stable structure; the corresponding electronic state is $X^3\Sigma^-$.

For $AlAs_2$, the lowest-energy structure is an isosceles triangle (C_{2v}), in which the Al atom is at the apex, the As–As distance (2.2955 Å) is longer than that of the As_2 dimer, and the bond length of the Al–As is 2.914 Å. It is a spin doublet and lower by 0.94 and 3.13 eV in energy than the quartet and sextet state. A bent chain with C_s ($^2A''$) symmetry in which Al takes a terminal position, and a linear structure ($C_{\infty v}$) in which Al takes central position, are two low-lying structures at, respectively, 0.42 and 0.49 eV above the most stable structure.

The lowest-energy structure of As_3 adopts linear structure ($D_{\infty h}$, $2\Pi_u$) as its global minimum. $AlAs_3$ is a rhombus with C_{2v} symmetry. The singlet isomer with $^1A_1$ is lower in total energy than the triplet and quintet isomers by 0.34 and 2.01 eV, respectively. Therefore, the spin singlet configuration is the most stable structure. Two dis-

Table 2
The symmetries (sym), the spin multiplicities (multi), and the total energies (E_t, hartree/particle) of the most stable and low-lying $AlAs_n$ ($n = 1$–15) clusters.

Cluster	Sym	Multi	E_t	Cluster	Sym	Multi	E_t
AlAs	$C_{\infty v}$	3	−8.0551	$AlAs_9$	C_1	1	−57.2041
$AlAs_2$	C_{2v}	2	−14.2155	$AlAs_{10}$	C_1	2	−63.3387
$AlAs_3$	C_{2v}	1	−20.3517	$AlAs_{11}$	C_1	1	−69.4772
$AlAs_4$	C_{2v}	2	−26.5018	$AlAs_{12}$	C_1	2	−75.6270
$AlAs_5$	C_{5v}	1	−32.6635	$AlAs_{13}$	C_1	1	−81.7681
$AlAs_6$	C_s	2	−38.7817	$AlAs_{14}$	C_1	2	−87.8952
$AlAs_7$	C_s	1	−44.9355	$AlAs_{15}$	C_1	1	−94.0647
$AlAs_8$	C_s	2	−51.0542				

torted tetrahedrons with C_s symmetries are low-lying structures lying 0.25 and 0.47 eV higher in energy.

The arsenic tetramer has the tetrahedral (T_d) structure. In the case of $AlAs_4$, four low-lying nearly degenerate structures are found, three of which are 3D structure and the other one is the pentagon configuration with the impurity Al atom at its vertex position, which is the most stable structure. The doublet isomer is more stable than other spin states, in that the total energy of the doublet is lower by 1.29 and 2.31 eV than that of quartet and sextet isomers. And the 3D (C_{2v}, $^2A_1$) isomer, the C_s ($^2A''$) structure and the square pyramid (C_{4v}, $^2A_1$) are three low-lying isomers, which are above the lowest-energy structure by 0.05, 0.34 and 0.53 eV, respectively.

For As_5, the most stable structure with C_{2v} symmetry is a tetrahedral As_4 structure with a twofold atom bond to it. The first three-dimensional (3D) structure of $AlAs_n$ occurs at $n = 5$. The lowest-energy structure for $AlAs_5$ is with C_{5v} symmetry, which is derived from the As_5 cluster by placing a fivefold Al atom on the top. The next energy minimum with C_s symmetry is 0.44 eV above the ground state. The other low-lying structure with the lower C_s ($^1A'$) symmetry is a distorted triangle prism lying 1.08 eV higher in energy. It is built from substitution of an As atom by an Al atom in the triangle prism As_6. Another C_s ($^1A'$) structure by capping an additional Al atom between two As atoms in structure of As_5 has an energy 1.47 eV less stable.

As for As_6, the lowest-energy structure is a prism structure with D_{3h} ($^1A'_1$) symmetry. The $AlAs_6$ (C_s) derived from a boat-shape As_6 by the adding of 1 twofold Al atom between As atoms. Moreover, the doublet isomer with electronic state $^2A'$ is lower in total

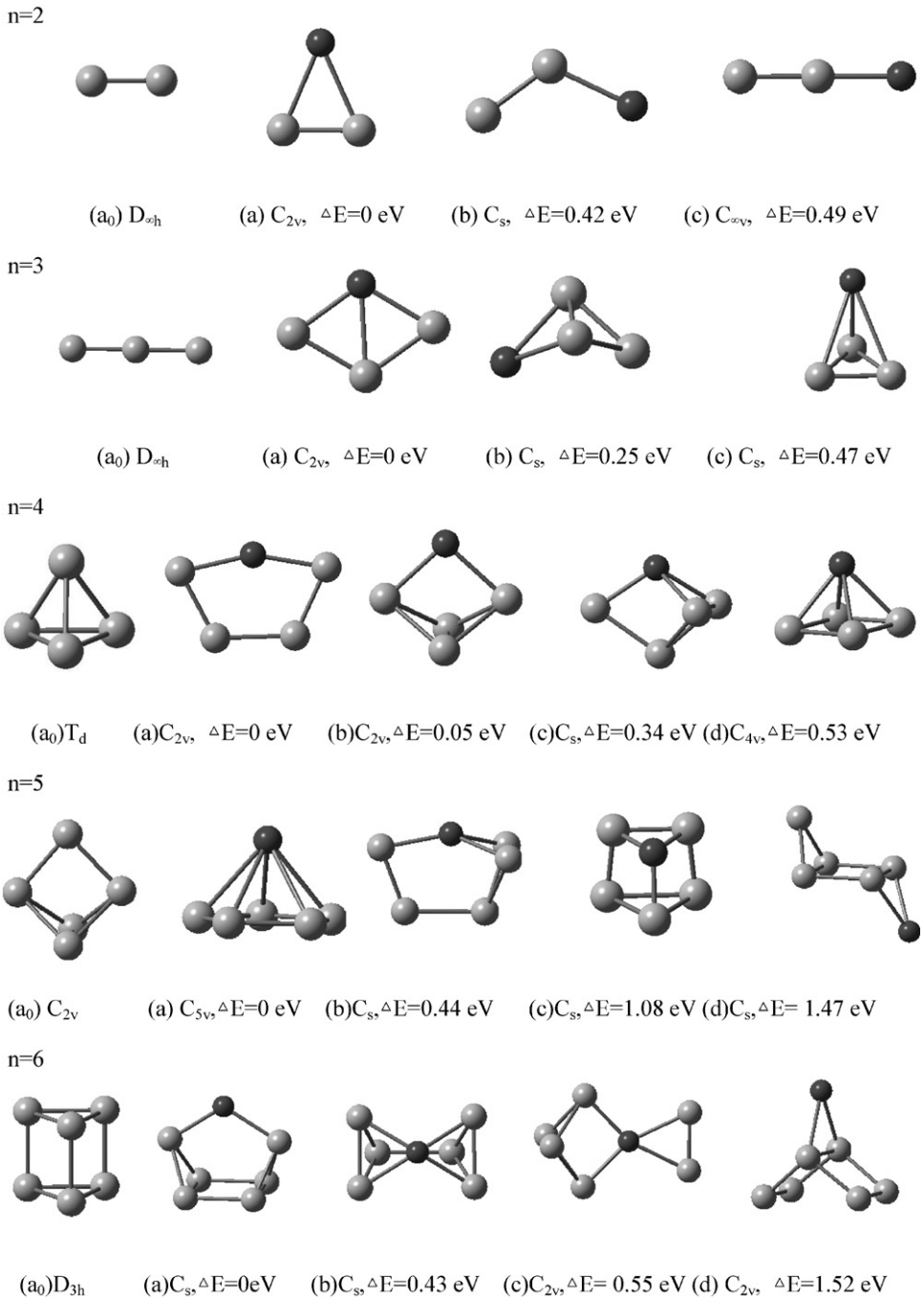

Fig. 1. Lowest-energy and low-lying structures of $AlAs_n$ ($n = 1$–15) clusters and lowest-energy structures of As_n ($n = 2$–16) clusters. The black and gray balls represent As and Al atoms, respectively.

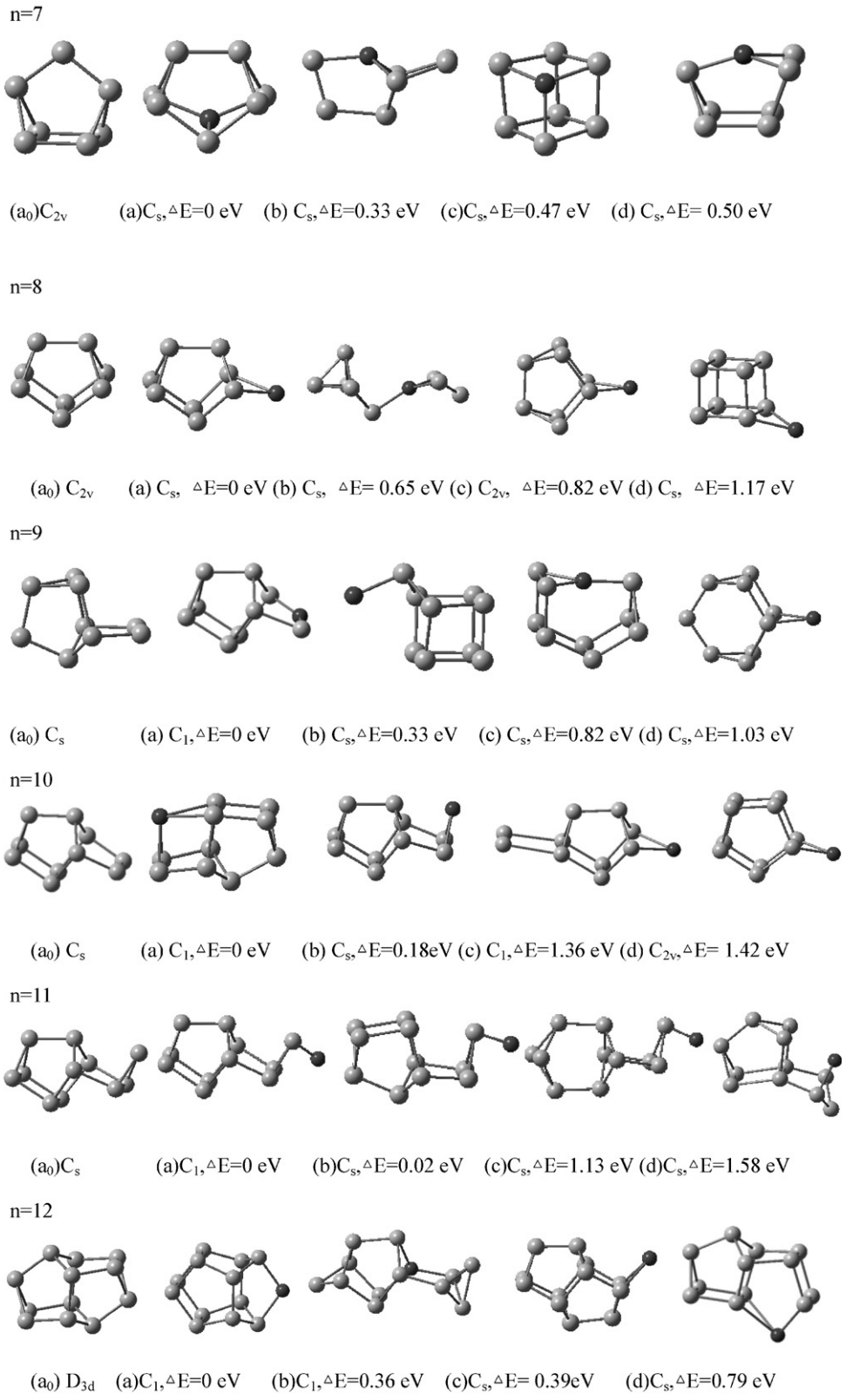

Fig. 1. (*Continued*)

energy than the quarter and sextet isomers by 2.12 and 3.16 eV, respectively. Next in the energy ordering is found to be face-capped triangle prism with C_{2v} ($^2A_2$) symmetry in our present optimization. It can be viewed as capping an additional Al atom on the square face of the triangle prism As_6. Two As–As bonds are broken in the capping procession. It locates at 0.43 eV above the ground state. Two structures with both C_{2v} symmetries are lying 0.55 and 1.52 eV, respectively, higher in energy.

In the case of $n = 7$, the pure As_7 has the similar geometry as the $AlAs_6$ with C_{2v} ($^2B_1$) symmetry. The present calculations consider a cuneane structure as the ground state of $AlAs_7$ cluster, which can be derived from a square-face-capped triangle prism As_7 by adding an

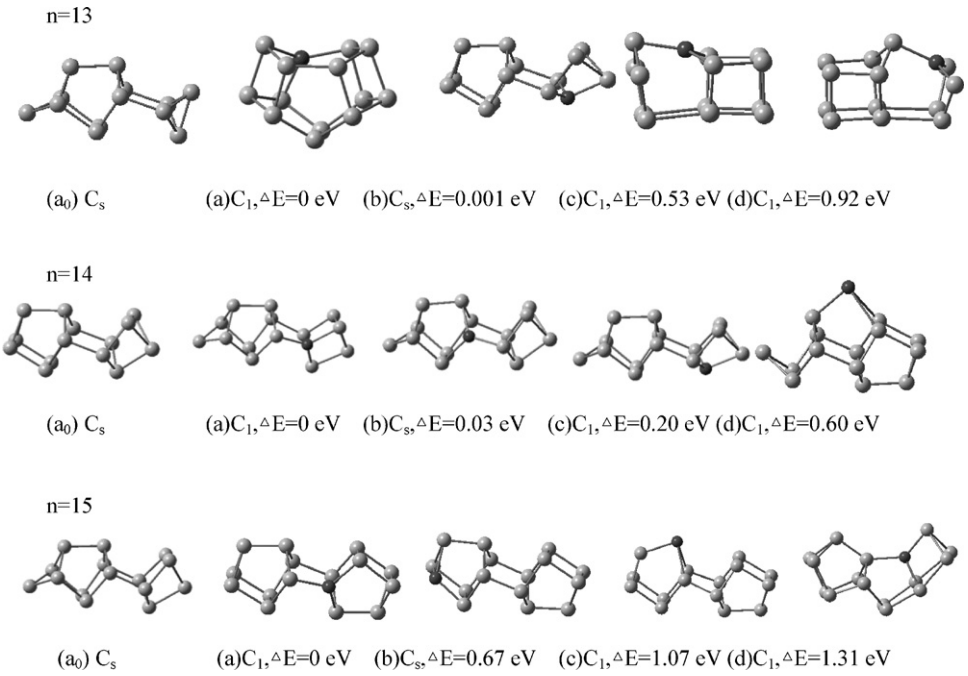

Fig. 1. (*Continued*).

additional threefold Al atom. The symmetry of As_7 is changed from C_{2v} to lower C_s symmetry of $AlAs_7$ in the procession. Moreover, the singlet isomer with electronic state $^1A'$ is lower in total energy than the triplet and quintet isomers by 0.93 and 2.15 eV, respectively. Therefore, the spin singlet configuration is the most stable structure. Another C_s form with the $^1A'$ state is a low-lying structure with higher energy 0.33 eV. The third $AlAs_7$ isomer in the energy ordering is a distorted cube structure with C_s ($^1A'$) symmetry lying 0.47 eV above the ground state, which is obtained by substitution of one As atom by one Al atom in the cube As_8. Another C_s form with the same electronic states as the ground state lies 0.50 eV higher in energy.

The lowest-energy structure of As_8 is a cuneane structure with the symmetry of C_{2v} ($^1A_1$). The most stable geometry of $AlAs_8$ is the result of the addition of the Al atom to the lowest-energy structure of As_8 cluster. Moreover, the doublet structure is lower in total energy than the quartet and sextet isomers by 1.26 and 2.12 eV, indicating that the doublet is more stable than other spin states, the corresponding electronic state is $^2A''$. The C_s symmetry structure with Al impurity at its center is higher by 0.65 eV. Al capped another different position of As_8 cluster yields the other low-lying structure, which is 0.82 eV higher in energy.

The lowest-energy structures I found for As_9 is with C_s symmetry, which may be viewed as a dimer attached to the most stable form of As_7 and have been confirmed to be lower in energies with no imaginary frequencies. For $AlAs_9$ cluster, the ground-state geometry is the Al atom substitute one capping As atom of As_{10} with C_1 symmetry. The total energy of the ground-state geometry with spin singlet is lower by 0.35 and 1.50 eV than spin triplet and quintet isomers. Therefore, the spin singlet form is the most stable structure. The structures of isomer (b), (c), (d) all with spin singlet and with the same C_s symmetries are above the lowest-energy structure by 0.33, 0.82, 1.03 eV, respectively.

Adding two As atoms in the same side of cuneane As_8, I obtain the ground state of As_{10}. The ground-state geometry of $AlAs_{10}$ cluster with C_1 symmetry can also be seen as substitutional structure of As_{11}. The form (a) with spin doublet is lower in total energy by 0.79 and 2.41 eV than spin quartet and sextet isomers. Therefore, the structure (a) with spin doublet is the most stable structure. Other isomers (b), (c) and (d) could be seen as the Al atom capped on the different positions of As_{10} and are 0.18, 1.36 and 1.42 eV higher in energy.

The most stable structure of As_{11} is the C_s form. By capping Al atom in the edge of the As_{11}, I could obtain the low-lying geometry of $AlAs_{11}$ with C_1 symmetry. The optimized results indicate that the singlet spin state is lower in total energy than the triplet and quintet isomers by 1.38 and 2.56 eV, respectively. Three low-lying geometries (b), (c), (d) of $AlAs_{11}$ all with C_s symmetries are 0.02, 1.13, and 1.59 eV, respectively higher in energy.

As_{12} cluster has the D_{3d} structure, which can be seen as two cuneane As_8 binding with four same As atoms. The ground-state structure of $AlAs_{12}$ is with C_1 symmetry which has the same building model as As_{12} cluster. Moreover, the total energy of $AlAs_{12}$ with spin doublet is lower by 0.74 and 2.45 eV than spin quartet and sextet isomers. The middle As atom substituting by the impurity Al atom could get the low-lying structure (b), 0.36 eV higher than structure (a). Other two low-lying geometries (c) and (d) of $AlAs_{12}$ all with C_s symmetries are 0.39 and 0.79 eV, respectively higher in energy.

As_{13} takes the C_s structure as its ground state. The most stable $AlAs_{13}$ is with C_1 symmetry. Furthermore, the total energy of structure (a) with spin singlet state is lower than those of the triplet and quintet isomers by 1.14 and 1.53 eV, respectively. The structure of isomer (b) with C_s symmetry is above the lowest-energy structure by only 0.001 eV in energy, which could be seen as substitute one As atom by Al atom at the edge of As_{14}. The structures c and d are 0.53 and 0.92 higher in energy.

The most stable structure of As_{14} is the C_s ($^1A'$) form, which can be seen as the combination of As_8 and As_6. For $AlAs_{14}$ cluster, the ground-state geometry (a) is the Al atom that falls into the center of As_{15} with C_1 symmetry. The total energy of (a) with spin doublet is lower by 0.35 and 0.67 eV than spin quartet and sextet isomers. Another low-lying isomers (b) and (c) with the same C_1 symmetries are also the Al atom falling the different positions of the As_{15} cluster. Their energy differences are 0.03 and 0.20 eV.

The optimized structure of neutral As_{15} is with C_s ($^2A'$) symmetry. The ground-state geometry of $AlAs_{15}$ cluster with C_1 symmetry can be seen as substitutional structure of As_{16} with Al impurity

replacing the center As atom in the As_{16} cluster. The total energy of (a) with spin singlet is lower by 1.39 and 2.63 eV than those of spin triplet and quintet isomers. Other isomers (b) and (c) are the Al atom capping the outside As atom in the As_{16} clusters, which is 0.67 and 1.07 eV higher in energy.

In summary, the Al impurity in the most stable structures of $AlAs_n$ (n = 6–15) clusters can be looked upon as a substitutional Al impurity in the pure As_{n+1} clusters (for example $AlAs_6$, $AlAs_7$, $AlAs_9$, $AlAs_{14}$ and $AlAs_{15}$ clusters) or capping the different sides of the low-lying geometry of As_n clusters (for example $AlAs_8$, $AlAs_{10}$, $AlAs_{11}$, and $AlAs_{12}$ clusters). For small clusters, the Al atom prefer to occupy a peripheral position, and from $n > 12$ clusters, the Al atom completely falls into the center of the As frame. The above growth pattern is not suitable for $AlAs_n$ (n = 1–5, 13) clusters.

The energy surface of a large molecule can be rather complex and there could be other stable minimums corresponding to geometries that are unexplored. Although the isomers of $AlAs_n$ have been studied extensively and reported in this letter, there can be no guarantee that other possible minima do not exist. My results of geometry optimization are only predictions, and it would be of great interest to see more experimental and theoretical studies being done on these systems.

3.2. Stabilities and electronic properties

I now discuss the relative stability of these clusters by computing the energy that is indicative of the stability. I compute the atomization or binding energy (E_b) per atom, the dissociation energy (ΔE) for an As atom, and the second-order energy differences ($\Delta_2 E$) as, respectively,

$$E_b[AlAs_n] = \frac{nE[As] + E[Al] - E[AlAs_n]}{n+1}, \quad (1)$$

$$\Delta E[AlAs_n] = E[AlAs_{n-1}] + E[As] - E[AlAs_n], \quad (2)$$

$$\Delta_2 E[AlAs_n] = E[AlAs_{n+1}] + E[AlAs_{n-1}] - 2E[AlAs_n] \quad (3)$$

In general the E_b increases sharply for very small clusters and then follows a plateau as the cluster size grows. Small humps or dips for the specific size of clusters signify their relative stabilities. The E_b of the $AlAs_n$ clusters (shown in Fig. 2) is calculated using the Eq. (1), where E(As), E(Al), and E($AlAs_n$) represent the energies of an As atom, an Al atom, and the total energy of the $AlAs_n$ cluster, respectively. For comparison, I also plot the E_b of the host As_n cluster, $E_b[As_n] = (nE[As] - E[As_n])/n$, in Fig. 2. As seen in this figure, the average binding energies of the most $AlAs_n$ clusters are higher than those of the pure As_n clusters (except for n = 2 and 12).

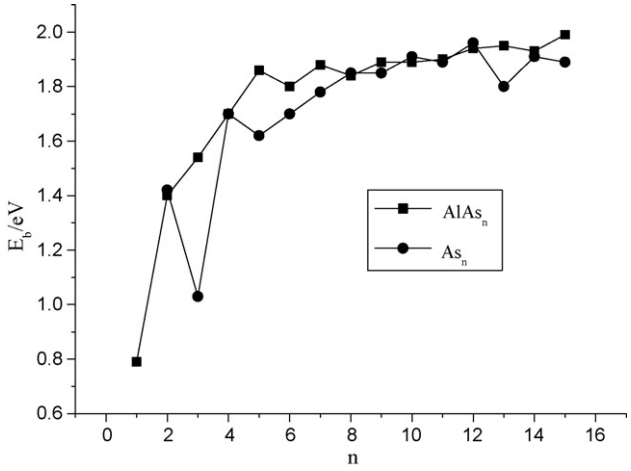

Fig. 2. The binding energy per atom of $AlAs_n$ and As_n clusters.

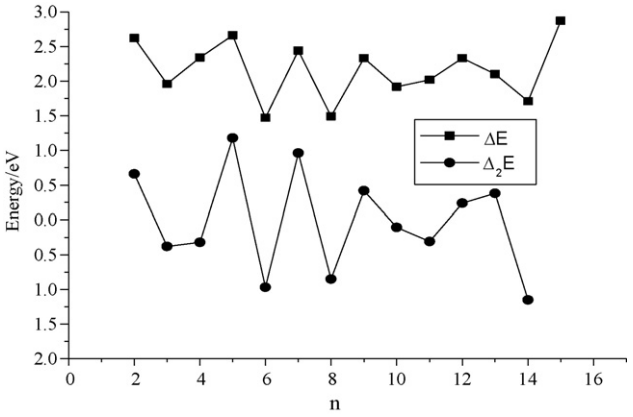

Fig. 3. The second-order energy difference $\Delta_2 E$ and the dissociation energy ΔE of the $AlAs_n$ (n = 2–15) clusters.

It indicates that the doped Al atom in the As_n clusters contributes to strengthen the stabilities of the As framework. For $AlAs_n$, the E_b evolves monotonically with total number of atoms in the cluster. Especially, for n = 1–5, the E_b increases rapidly from 0.79 eV for AlAs to 1.86 eV for $AlAs_5$ which corresponds to the structure transition from two to three dimension. The E_b increases gradually in the range n = 6–15, in which the rate of increase becomes weak (only from 1.80 to 1.99 eV). In addition, the comparison of As with the BE curve for $AlAs_n$ clusters shows that the small clusters of $AlAs_n$ are strongly bound. As the cluster grows in size, the difference between the BE curves of $AlAs_n$ clusters and pure As clusters steadily diminishes, indicating that the bonding in doped clusters is essentially similar to that in pure clusters.

In cluster physics, the dissociation energy (ΔE) and the second-order energy differences ($\Delta_2 E$) are sensitive quantities that reflect the relative stability of the investigated clusters. The ΔE shows the energy that one atom is separated from the host clusters. The $\Delta_2 E$ is often compared directly with the relative abundances determined in mass spectroscopy experiments. They are defined as Eqs. (2) and (3). Where $E(AlAs_n)$, $E(AlAs_{n+1})$, $E(AlAs_{n-1})$, and E(As) represent the total energies of the most stable $AlAs_n$, $AlAs_{n+1}$, and $AlAs_{n-1}$ clusters and an As atom, respectively. As shown in Fig. 3, particularly prominent maxima of $\Delta_2 E$ are found at n = 2, 5, 7, 9, 12, and 13 indicating higher stability than their neighboring clusters. It is observed that, for the $AlAs_n$ cluster, the ΔE of $AlAs_2$ (2.62 eV), $AlAs_5$ (2.66 eV), $AlAs_7$ (2.44 eV), $AlAs_9$ (2.33 eV), $AlAs_{12}$ (2.33 eV) and $AlAs_{15}$ (2.87 eV) clusters are higher than other clusters. Thus I can conclude that the magic clusters are found at n = 2, 5, 7, 9, 12, and 15 for $AlAs_n$.

I have also calculated the dissociation energy for Al atom, i.e., the energy released upon adsorption of Al by a pure As cluster, according to

$$E_{de} = E[As_n] + E[Al] - E[AlAs_n] \quad (4)$$

The calculated values of E_{de} for the clusters up to $AlAs_{15}$ ranges between 1.36 and 3.84 eV (Table 3). The minimum value (1.36 eV) occurs for $AlAs_2$, while it takes the maximum value (3.84 eV) for $AlAs_{13}$.

The HOMO–LUMO gap (highest occupied-lowest unoccupied molecular orbital gap) is a useful quantity for examining the stability of clusters. It is found that systems with larger HOMO–LUMO gaps are, in general, less reactive. In the case of an odd-electron system, I calculate the HOMO–LUMO gap as the smallest spin-up–spin-down gap. The HOMO–LUMO gaps as thus calculated are presented in Fig. 4. For $AlAs_n$ clusters, local peaks are found at n = 2, 5, 7, 9, 11, 13, and 15 implying the chemical stability of these clusters is stronger than that of their neighboring clusters. I note that

Table 3
The dissociation energy for Al atom (in electron volt) (see text for full details) calculated at B3LYP/lanl2dz level.

	Cluster							
	AlAs	$AlAs_2$	$AlAs_3$	$AlAs_4$	$AlAs_5$	$AlAs_6$	$AlAs_7$	$AlAs_8$
E_{ad}	1.58	1.36	3.07	1.71	3.04	2.44	2.60	1.79
	Cluster							
	$AlAs_9$	$AlAs_{10}$	$AlAs_{11}$	$AlAs_{12}$	$AlAs_{13}$	$AlAs_{14}$	$AlAs_{15}$	
E_{ad}	2.20	1.74	2.05	1.65	3.84	2.18	3.49	

the HOMO–LUMO gaps of $AlAs_n$ (n = 4–15) present a similar oscillating behavior as observed for the dissociation energy and the second-order energy differences. Clusters with an even number of electrons have a larger HOMO–LUMO energy gap and therefore are expected to be less reactive than clusters with an odd number of electrons. The stability exhibited by even number of electrons clusters is due to their closed-shell configurations that always come along with an extra stability. It is important to mention that this result is agreement with the electronic shell jellium model [22], where filled-shells cluster with 2, 8, 18, 20, 40, 58, 92, ... valence electrons have increased stability, the mass spectra of cluster distribution shows pronounced intensity in clusters with these number of atoms, the so-called magic numbers.

Experimentally, the electronic structure is probed via measurements of ionization potentials, electron affinities, polarizabilities, etc. Therefore, I also study these quantities to understand their evolution with size. These quantities are determined within B3LYP for the lowest-energy structures obtained within the same scheme.

The vertical ionization potential (VIP) is calculated as the self-consistent energy difference between the cluster and its positive ion with the same geometry. The VIP is plotted in Fig. 5 as a function of cluster size. The corresponding data are given in Table 4. In general, the VIP decreases as the cluster size increases. The peaks occurring at $AlAs_n$ (n = 2, 5, 7, 13, 14, and 15) are prominent, with large drops for the following clusters. Also shown in Fig. 5 are the VIPs of pure arsenic clusters. These have also been calculated at the B3LYP/lanl2dz level of theory, with structures optimized at the same level of theory. The comparison of the two curves shows that odd–even oscillations are not observed in $AlAs_n$ clusters in the whole, while in pure As clusters, the VIP exhibits odd–even pattern in the range of n = 2–7, 10–15.

I have also calculated vertical electron affinities (VEA) for these clusters (see Fig. 6 and Table 4) by assuming the geometry for the charged cluster to be the same as for the neutral one. The VEA exhibits an odd–even pattern from n = 5. This is a consequence of the electron pairing effect. In the case of clusters with an even number of valence electrons, the extra electron has to go into the next orbital, which costs energy, resulting in a lower value of VEA.

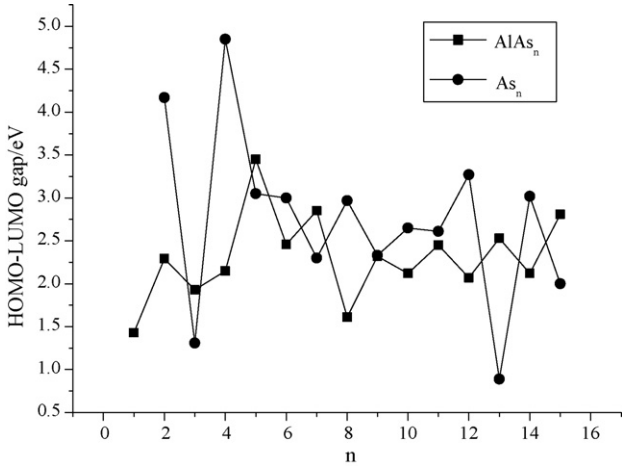

Fig. 4. The HOMO–LUMO gap of the $AlAs_n$ and As_n clusters.

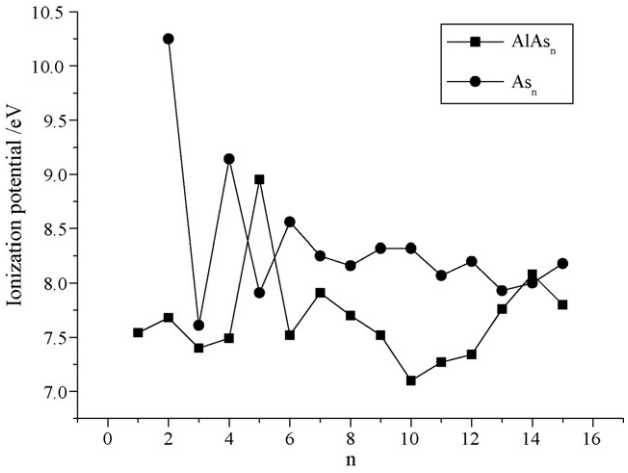

Fig. 5. Ionization potential for $AlAs_n$ and As_n clusters.

Another useful quantity is the chemical hardness [23], which can be approximated as

$$\eta \approx \frac{1}{2}(I - A) \approx \frac{1}{2}(\varepsilon_L - \varepsilon_H), \quad (5)$$

where A and I are the electron affinity and ionization potential, ε_L and ε_H are the energies of the highest occupied molecular orbital (HOMO) and the lowest unoccupied molecular orbital (LUMO), respectively. Chemical hardness has been established as an electronic quantity that in many cases may be used to characterize the relative stability of molecules and aggregate through the principle of maximum hardness (PMH) proposed by Pearson [24]. The

Table 4
Vertical ionization potential (VIP) and vertical electron affinities (VEA) of $AlAs_n$ (n = 1–15) clusters at B3LYP/lanl2dz level.

Cluster	VIP (eV)	VEA (eV)
AlAs	7.54	1.74
$AlAs_2$	7.68	1.75
$AlAs_3$	7.40	1.82
$AlAs_4$	7.49	2.56
$AlAs_5$	8.95	1.67
$AlAs_6$	7.52	2.38
$AlAs_7$	7.91	1.95
$AlAs_8$	7.70	2.93
$AlAs_9$	7.52	2.34
$AlAs_{10}$	7.10	2.56
$AlAs_{11}$	7.27	2.13
$AlAs_{12}$	7.34	2.88
$AlAs_{13}$	7.76	2.57
$AlAs_{14}$	8.08	3.16
$AlAs_{15}$	7.80	2.55

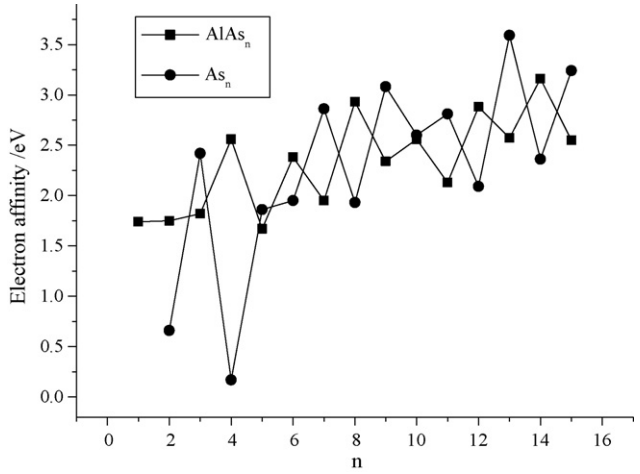

Fig. 6. Electron affinity for $AlAs_n$ and As_n clusters.

PMH asserts that molecular systems at equilibrium present the highest value of hardness. The hardness of $AlAs_n$ clusters, calculated according to Eq. (5) using VIP for the ionization potential and VEA for the electron affinity, is shown in Fig. 7. Assuming that the PMH holds in these systems, I expect the hardness to present an oscillating behavior with local maxima at the clusters with even valence-electron clusters from $n = 5$, as found for the relative energy in Fig. 3, HOMO–LUMO gap in Fig. 4, VIP in Fig. 5 and VEA in Fig. 6. Fig. 7 shows that the even valence-electron clusters from $n = 5$ present higher values of hardness than their neighboring clusters. I do observe the even–odd oscillating feature similar to that already stressed in the HOMO–LUMO, VIP, VEA, and stability criteria. Stable clusters are harder than their neighbors' odd valence-electron systems.

I present in Table 5 the static mean polarizability $\langle\alpha\rangle$ and mean polarizability per atom ($\langle\alpha\rangle/n+1$) for the lowest-energy structures calculated within the B3LYP scheme. The static mean polarizability $\langle\alpha\rangle$ is calculated from the polarizability tensor components as

$$\langle\alpha\rangle = \frac{1}{3}(\alpha_{xx} + \alpha_{yy} + \alpha_{zz}) \quad (6)$$

The static polarizability represents one of the most important observables for the understanding of the electronic properties of clusters, it is proportional to the number of electrons of the systems, and it is very sensitive to the delocalization of valence electrons as well as to the structure and shape of the system.

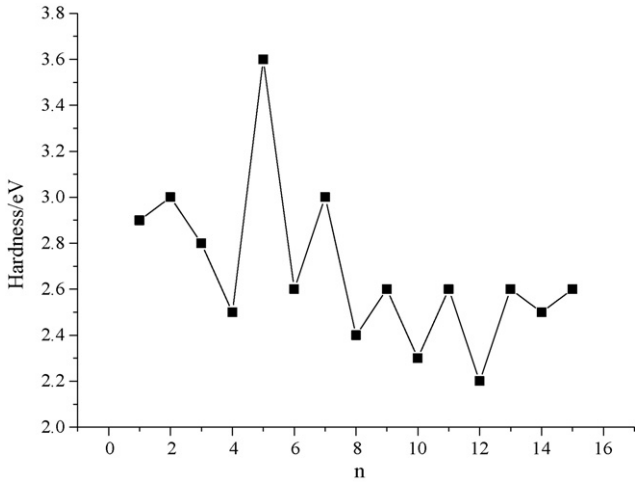

Fig. 7. Hardness of $AlAs_n$ clusters.

Table 5
Static mean polarizability $\langle\alpha\rangle$ and mean polarizability per atom ($\langle\alpha\rangle/n+1$) of $AlAs_n$ ($n = 1$–15) clusters calculated at B3LYP/lanl2dz level. All values are in a.u.

Cluster	α_{xx}	α_{yy}	α_{zz}	$\langle\alpha\rangle$	$\langle\alpha\rangle/n+1$
AlAs	787.0	36.6	107.4	310.3	155.2
$AlAs_2$	46.6	106.8	135.2	96.2	32.1
$AlAs_3$	46.9	180.6	130.5	119.3	29.8
$AlAs_4$	56.6	229.9	187.7	158.1	31.6
$AlAs_5$	194.6	194.6	160.0	183.1	30.5
$AlAs_6$	192.4	219.5	232.9	214.9	30.7
$AlAs_7$	226.2	214.3	271.4	237.3	29.7
$AlAs_8$	324.1	289.6	254.5	289.4	32.2
$AlAs_9$	394.6	281.0	239.3	305.0	30.5
$AlAs_{10}$	426.6	323.6	294.4	348.2	31.7
$AlAs_{11}$	614.4	303.4	294.0	403.9	33.7
$AlAs_{12}$	466.8	355.0	335.4	385.7	29.7
$AlAs_{13}$	462.6	394.1	373.1	409.9	29.3
$AlAs_{14}$	710.7	380.7	357.7	483.0	32.2
$AlAs_{15}$	739.6	400.0	392.2	510.6	31.9

In Table 5 I note that when going from $AlAs_2$ to $AlAs_{10}$ and $AlAs_{12}$ to $AlAs_{15}$ the polarizability of the clusters increases monotonically showing the expected proportionality with n (or the total number of electrons). It is also evident from Table 5 that the odd–even oscillations, which are present in the dissociation energy, the second-order energy differences, HOMO–LUMO gap, VEA, and hardness, are seen here except for $AlAs_{11}$ with the largest value (33.7 a.u.).

4. Summary and conclusions

Arsenic clusters doped with a single Al impurity atom has been studied by an all-electron linear combination of atomic orbital approach, within spin-polarized density-functional theory, using the GGA scheme for the exchange-correlation. The Al impurity of the lowest-energy geometries of $AlAs_n$ ($n = 1$–12) is found to occupy a peripheral position, while the Al impurities of $AlAs_n$ ($n = 13$–15) prefer to occupy internal sites in the arsenic clusters. The stability of the lowest-energy structures is investigated by analyzing energies. Odd–even oscillations of $AlAs_n$ cluster from $n = 5$ are observed in most of the physical properties investigated. The stability analysis based on the energies and the physical properties clearly shows the $AlAs_n$ cluster from $n = 5$ with an even number of valence electrons are more stable than clusters with odd number of valence electrons.

Acknowledgments

This work was financially supported by the National Natural Science Foundation of China (Grant No. 20603021), Youth Foundation of Shanxi (Grant No. 2007021009) and the Youth Academic Leader of Shanxi.

References

[1] P. Ballone, R.O. Jones, J. Chem. Phys. 100 (1994) 4941.
[2] M. Shen, J. Chem. Phys. 101 (1994) 2261.
[3] R.K. Yoo, B. Ruscic, J. Berkowitz, J. Chem. Phys. 96 (1992) 6696.
[4] T.P. Lippa, S.J. Xu, S.A. Lyapustina, J. Chem. Phys. 109 (1998) 10727.
[5] L. Guo, J. Mater. Sci. 42 (2007) 9154.
[6] Z.Y. Liu, C.R. Wang, R.B. Huang, L.S. Zheng, Int. J. Mass Spectrom. 141 (1995) 201.
[7] W. Andreoni, Phys. Rev. B 45 (1992) 4203.
[8] H.K. Quek, Y.P. Feng, C.K. Ong, Z. Phys. D 42 (1997) 309.
[9] V. Tozzini, F. Buda, A. Fasolino, J. Phys. Chem. B 105 (2001) 12477.
[10] A. Costales, A.K. Kandalam, R. Franco, R. Pandey, J. Phys. Chem. B 106 (2002) 1940.
[11] E.F. Archibong, A. St-Amant, J. Phys. Chem. A 106 (2002) 7390.
[12] P.Y. Feng, D. Dai, K. Balasubramanian, J. Phys. Chem. A 104 (2000) 422.
[13] X. Zhu, J. Mol. Struct. (Theochem.) 638 (2003) 99.
[14] M. Deshpande, D.G. Kanhere, R. Pandey, Phys. Rev. A 71 (2005) 063202.
[15] D.L. Chen, W.Q. Tian, C.C. Sun, Phys. Rev. A 75 (2007) 013201.
[16] F.Y. Tian, Q. Jing, Y.X. Wang, Phys. Rev. A 77 (2008) 2008.

[17] M.J. Frisch, G.W. Trucks, H.B. Schlegel, G.E. Scuseria, M.A. Robb, J.R. Cheeseman, V.G. Zakrzewski, J.A. Montgomery, Jr., R.E. Stratmann, J.C. Burant, S. Dapprich, J.M. Millam, A.D. Daniels, K.N. Kudin, M.C. Strain, O. Farkas, J. Tomasi, V. Barone, M. Cossi, R. Cammi, B. Mennucci, C. Pomelli, C. Adamo, S. Clifford, J. Ochterski, G.A. Petersson, P.Y. Ayala, Q. Cui, K. Morokuma, D.K. Malick, A.D. Rabuck, K. Raghava-chari, J.B. Foresman, J. Cioslowski, J.V. Ortiz, B.B. Stefanov, G. Liu, A. Liashenko, P. Piskorz, I. Komaromi, R. Gomperts, R.L. Martin, D.J. Fox, T. Keith, M.A. Al-Laham, C.Y. Peng, A. Nanayakkara, C. Gonzalez, M. Challacombe, P.M.W. Gill, B. Johnson, W. Chen, M.W. Wong, J.L. Andres, C. Gonzalez, M. Head-Gordon, E.S. Replogle, J.A. Pople, Gaussian, Inc., Wallingford, CT, 2004.
[18] P.J. Hay, W.R. Wadt, J. Chem. Phys. 82 (1985) 270.
[19] S.N. Khanna, P. Jena, Phys. Rev. Lett. 69 (1992) 1664.
[20] K.P. Huber, G. Herzberg, Molecular Spectra and Molecular Structure. IV. Constants of Diatomic Molecules, Van Nostrand Reinhold, New York, 1979.
[21] K. Balasubramanian, J. Mol. Spectrosc. 121 (1987) 465.
[22] J. Akola, M. Manninen, H. Hakkinen, U. Landman, X. Li, L.S. Wang, Phys. Rev. B 62 (2000) 13216.
[23] R.G. Parr, R.G. Pearson, J. Am. Chem. Soc. 105 (1983) 7512.
[24] R.G. Pearson, Chemical Hardness: Applications from Molecules to Solids, Wiley–VCH, Weinheim, 1997.